UNIVERSITY OF CALIFORNIA
Santa Barbara

Photoelectron Energy Distributions in the Far Ultraviolet

STATUS REPORT

January 1965 - June 1965

Research Grant NSG 91-60, Supplement 3

NATIONAL AERONAUTICS AND SPACE ADMINISTRATION

AND

UNIVERSITY OF CALIFORNIA, SANTA BARBARA

William C. Walker, Principal Investigator
Associate Professor, Physics

and

Lanny R. Hughey, Research Assistant

ABSTRACT

Photoelectron Energy Distributions in the Far Ultraviolet

32882

Photoemission has recently been recognized as a useful technique for studying electronic properties of solids. The purpose of this work has been to develop the electronic and other experimental equipment needed to measure both the quantum yield and energy distributions of photoelectrons. The system which was developed permits the direct recording of energy distributions by measuring the a-c conductance of a photocell subjected to a retarding potential.

The system was tested by obtaining preliminary measurements of photoelectron energy distributions from electropolished indium for selected wavelengths between 500 Å and 2000 Å. The results indicate that accurate energy distributions can be measured for photocurrents as low as 10^{-11} amp. Since the electropolished indium was not atomically clean no detailed interpretation of the data was attempted. A previously unobserved peak at 7 eV in the energy distribution for 21.2 eV photons was found which does not correspond to any known maximum in the density of states.

Author

I. Introduction

There are many experimental techniques available for studying the electronic structure of solids. Studies of cyclotron resonance, the anomalous skin-effect, de Haas-van Alphen effect and others provide detailed information on states near the fermi surface. Soft x-ray emission and absorption measurements give information on some features of the band structure. Optical absorption and reflectivity measurements provide accurate values of transition energies and can be interpreted in detail if the general features of the energy bands are known.

Photoemission as a technique for studying electronic properties of solids has certain advantages over other methods as has been pointed out by Spicer and Simon (ref. 1). Since the energy of the photoelectrons can be measured after excitation, information concerning the energies of the initial and final states can be obtained. This information facilitates the interpretation of optical data in terms of the band structure especially when, as is the case for most materials, the band structure is understood only qualitatively. It is possible, in addition, to extract information on electron scattering since photoemission is a two-step process involving optical excitation and electron transport through the solid to the surface.

Photoemission measurements have not as yet been used extensively to investigate band structure in solids. Some studies have been made, however, of a few metals and several semiconductors using photoemission measurements as a source of information on the electronic structure of the materials studied. Gobeli and Allen have employed photoemission measurements to study both surface and volume states in silicon (ref. 2 and 3). Taft and Philipp have investigated potassium and cessium antimonide using these methods (ref. 4), Spicer has used photoemissive measurements to investigate the alkali-antimonides (ref. 5 and 6). Spicer and Simon have employed these techniques to study silicon (ref. 7). Recent work by the group at Stanford directed by Prof. Spicer has included that of Kindig who investigated cadmium sulfide (ref. 8) and Berglund who used photoemission to study band structure and electron-electron scattering in copper and silver (ref. 9).

The purpose of this work has been to develop the electronic and other experimental components needed to measure photoelectron energy distributions and quantum yields in the far ultraviolet. Since the light intensities available in the far ultraviolet are quite low, the magnitudes of the resultant photocurrents are also quite small (10^{-10} amp. or less). This feature places

stringent requirements on the electronic components utilized in measuring photoemissive properties.

In this work a retarding potential method was employed to measure photoelectron energy distributions. Let $N_\omega(E)$ be the number of electrons emitted per second with energies between E and E+dE by a photoemitter produced by photons of frequency ω. The photocurrent flowing when there is a potential V between an emitter and a collector of a spherical photocell is

$$I_\omega(V) = e\int_{-eV}^{\infty} N_\omega(E)dE$$

The small-signal conductance of the cell at voltage V_o is then

$$g_\omega(V_o) = \frac{dI_\omega(V)}{dV}\bigg|_{V_o} = e^2 N_\omega(-eV_o),$$

demonstrating that the energy distribution of photoelectrons can be found simply by measuring the small-signal conductance of the photocell as a function of the retarding potential (see Figure 1). This technique has been used recently by Spicer and co-workers with considerable success (ref. 8 and 9).

In the present study the emphasis was placed on developing a workable measuring system. Photoemissive measurements were made on indium metal in part to check the operation of the apparatus and in part because of intrinsic interest in indium as an example of a solid in which both far ultraviolet interband transitions and

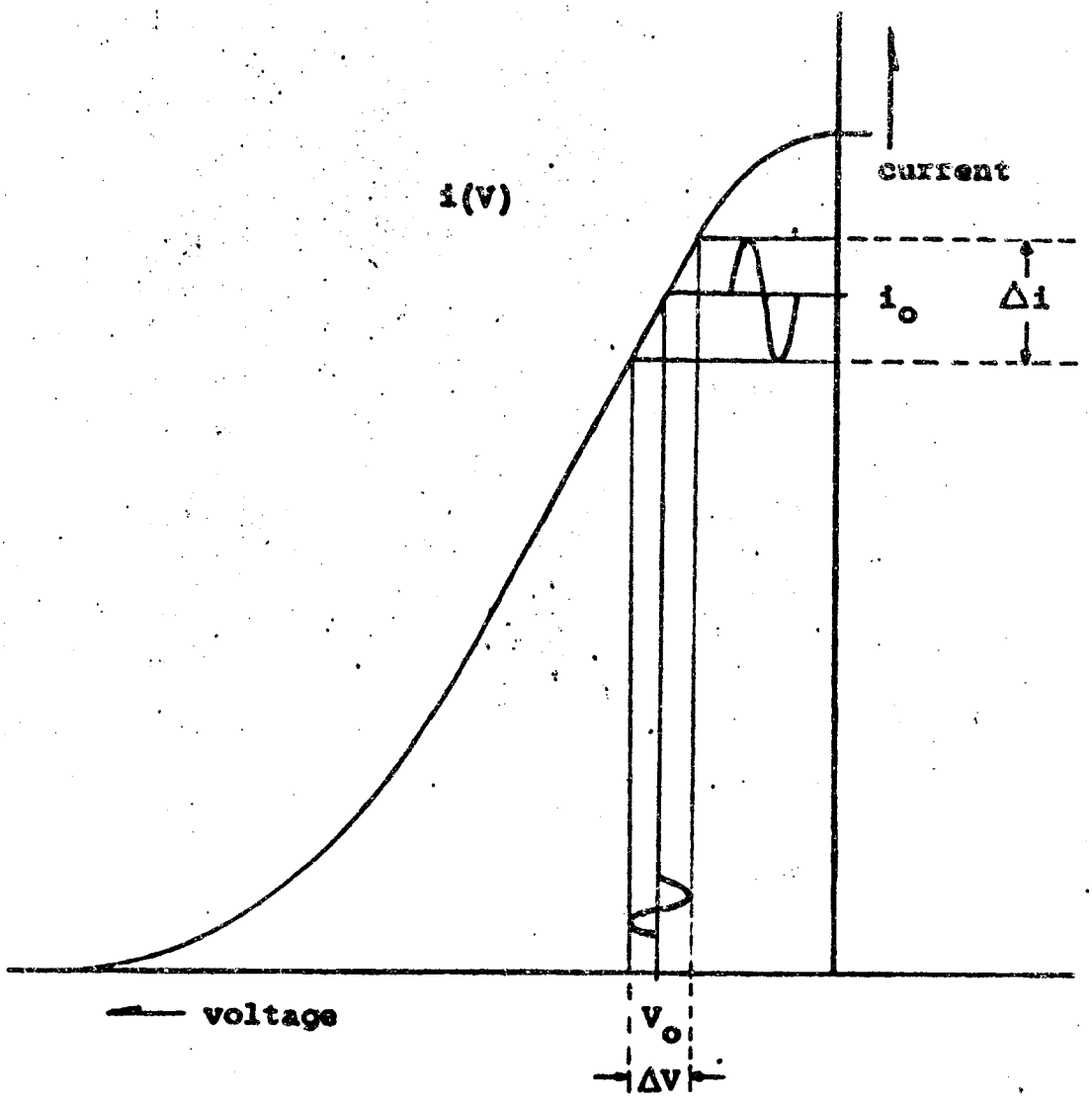

FIGURE 1. A graphical illustration of the a-c method of obtaining electron energy distributions. i(V) is a current vs. voltage curve for a typical photocell. With a voltage V_o applied to the cell there is a current i_o. If a small a-c voltage ΔV is added to the d-c voltage V_o the photocurrent will consist of i_o plus an a-c component Δi. If the amplitude of ΔV is held constant and V_o is changed slowly then Δi is proportional to the a-c conductance of the photocell, that is, it is proportional to the slope of the current vs. voltage curve.

plasmons constitute well defined forms of excitation.

The reflectivity, relative photoelectric quantum yield, and the photoelectron energy distributions of electro-polished indium were measured for photon energies ranging from 3 eV to 27 eV.

II. Experimental Apparatus and Procedures

A. The Photocell

Figure 3 shows a one-half scale diagram of the photocell. The collector consisted of a 400 ml pyrex round bottom flask with a 5/8" hole cut in the bottom end to admit the light beam and an auxiliary pumping throat blown into the neck of the flask. The neck was mounted on an aluminum disk with epoxy* and a strip of copper (½" x 1½" x .005") was mounted with epoxy inside the neck of the flask. An indium film, which served as the collector, was evaporated into the inner surface of the flask in a high vacuum evaporation chamber. Indium was used to minimize contact potential between the emitter and collector.

An indium sample was melted into the aluminum cup shown in Fig. 3 and was attached to a teflon mount. A spring clip which made the electrical connection via the strip of sheet copper, between the collector film and the kovar feed-through in the back plate of the sample holder was also attached to the teflon mount.

A Bayert-Alpert type ionization gauge was mounted in the rear plate of the photocell to permit measure-

---

*Hysol epoxy patch kit #1-C, Hysol Corporation, Los Angeles.

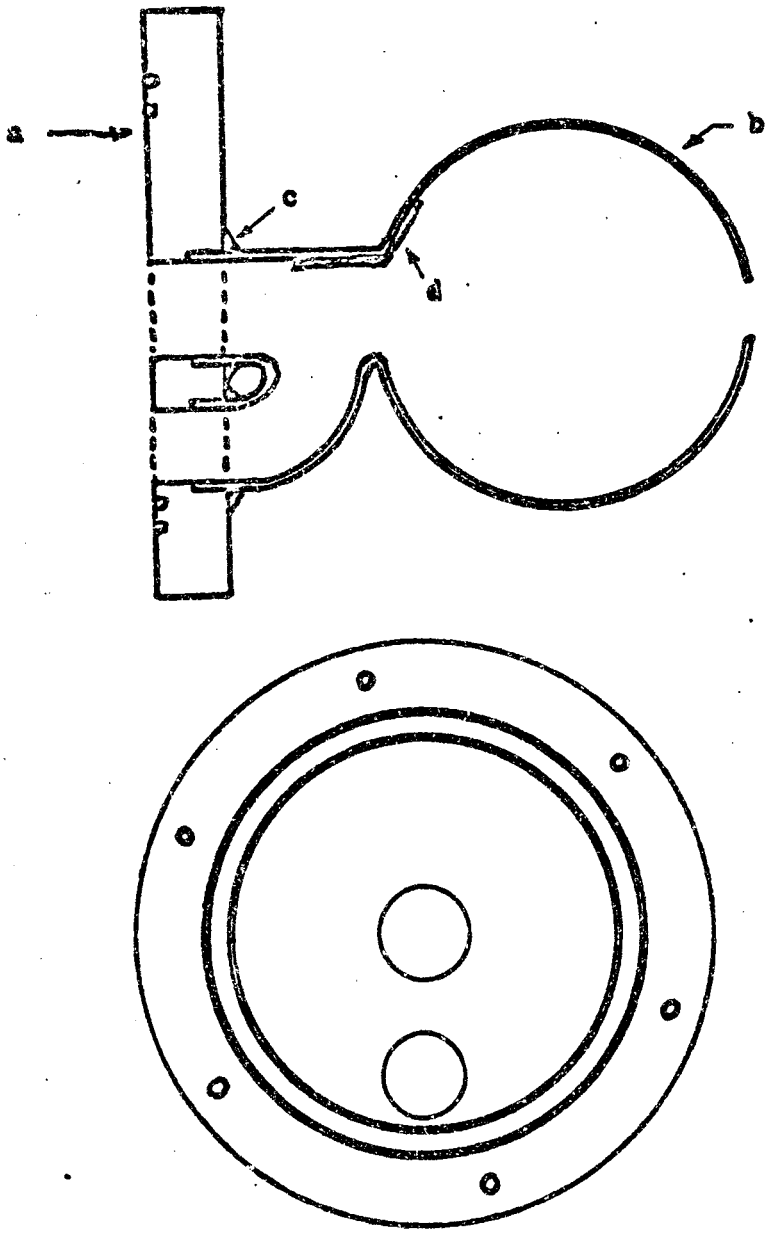

FIGURE 2. The photocell. a: Aluminum, b: pyrex flask, and c: epoxy. d: the sheet copper epoxied on the inside of the flask.

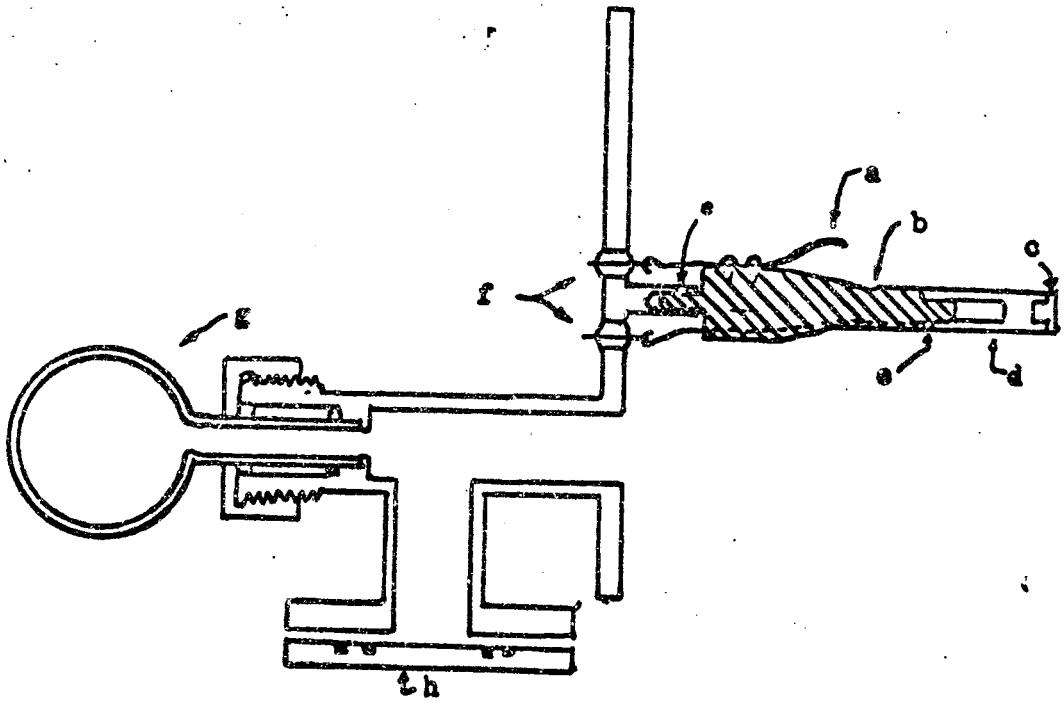

FIGURE 3. The sample holder and back plate of the photocell. a: spring clip collector lead, b: teflon mount, c: the indium sample, d: the aluminum sample holder, e: set screw fastening the holder to the teflon mount, f: kovar feed-throughs, g: ionization gauge and h: the blank-off plate for the auxiliary pumping port.

ment of the pressure in the cell under operating conditions. An additional pumping port was also located in the rear plate of the photocell which could be used in the event that the front end of the cell was sealed with a lithium fluoride or quartz window.

The photocell was mounted inside a stainless steel vacuum jacket which was attached to the light monitoring chamber as shown in Fig. 4. The light monitoring chamber bolted directly onto the monochromator exit slit housing and contained the light pipe photomultiplier unit as shown in Fig. 5.with which the incident light intensity was measured. The light pipe was made of 10mm pyrex rod which was heated and bent to the desired shape. The ends were polished to give a good optical surface. Sodium salicylate was dissolved in methanol and sprayed from an atomizer onto the bent end of the light pipe. The light pipe was heated somewhat before spraying on the sodium salicylate to speed up the evaporization of the methanol and to provide a smoother film.

B. Monochromator and Light Source

The photoelectric measurements were made using a McPherson model 225 one-meter normal incidence vacuum monochromator fitted with a 1200 lines/mm Bausch and Lomb grating capable of a dispersion of 8 A/mm. Supplementary reflectivity measurements were made with a Jarrell-

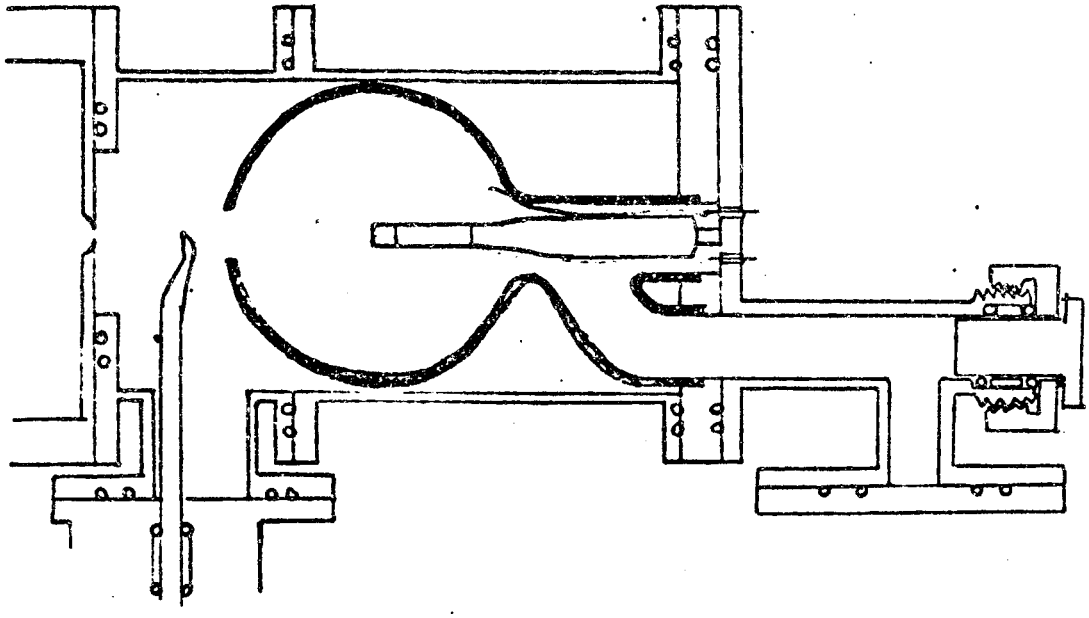

FIGURE 4. The assembled components of the photocell.

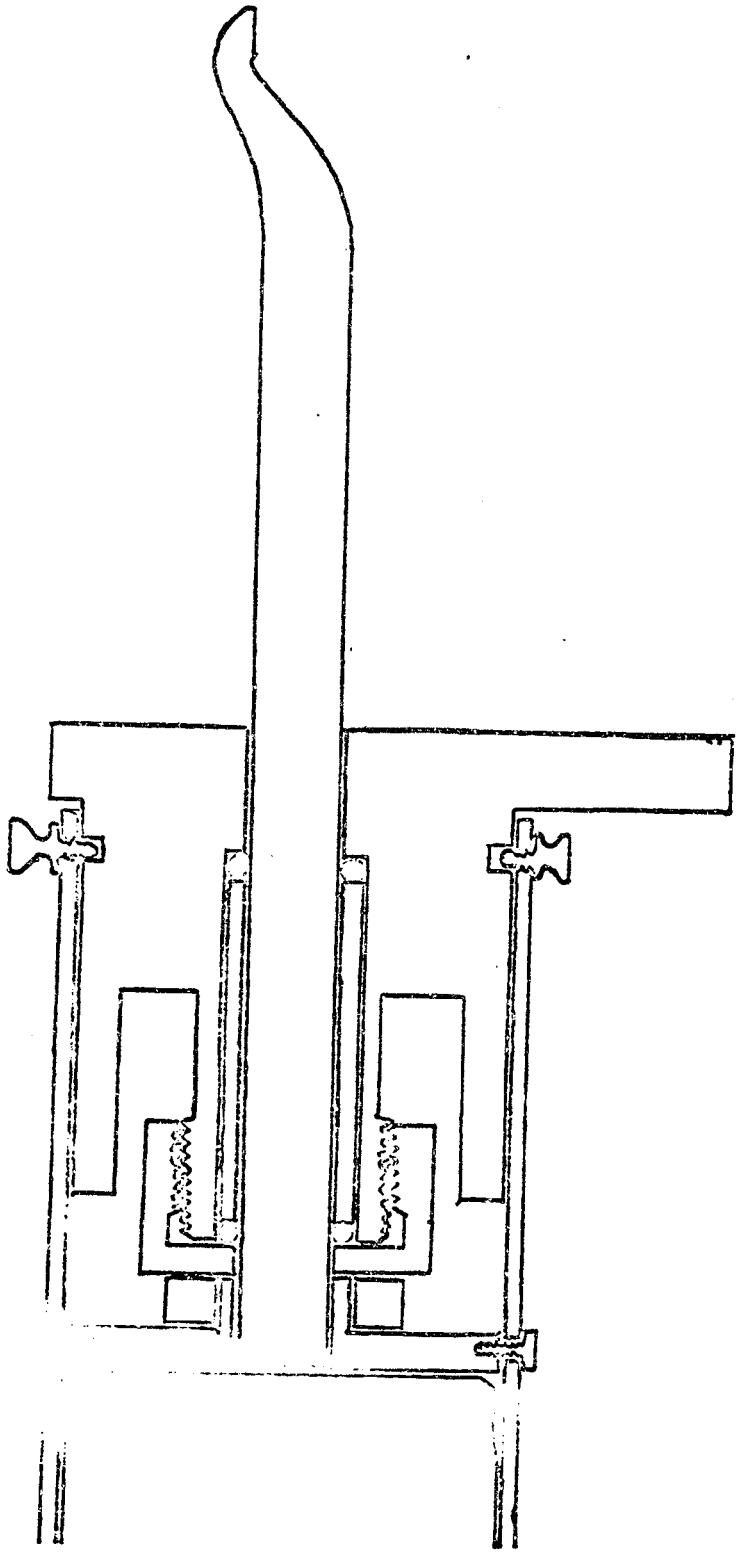

FIGURE 5. The photomultiplier light-pipe unit.

Ash model 78-650 one-half meter Seya-Namioka vacuum monochromator. The initial attempt to measure energy distributions using the Jarrell-Ash monochromator showed that the light output was inadequate for any but the most intense spectral lines.

The light source used in this work was developed by Professor W. C. Walker and is shown schematically in Fig. 6. The body of the light source was fused quartz and the water cooled capillary had a rectangular cross-section of approximately 1 mm by 3 mm. The tube was sealed to the entrance slit housing of the monochromator with a viton A o-ring which was compressed by a threaded cap. The water cooled 3/8" diameter electrodes were also sealed with o-rings. The electrodes were made of aluminum in order to minimize sputtering caused by ion bombardment and to retain good thermal conductivity. The grounded anode was located between the entrance slit and the cathode to keep positive ions from being accelerated toward the grating. The ends of both electrodes were well below the optical path from the capillary to the grating to reduce the amount of electron bombardment of the grating and to eliminate the sputtering of eletrode material onto the grating.

In this work, the light source was operated in a d-c mode to reduce electrical noise in the sensitive

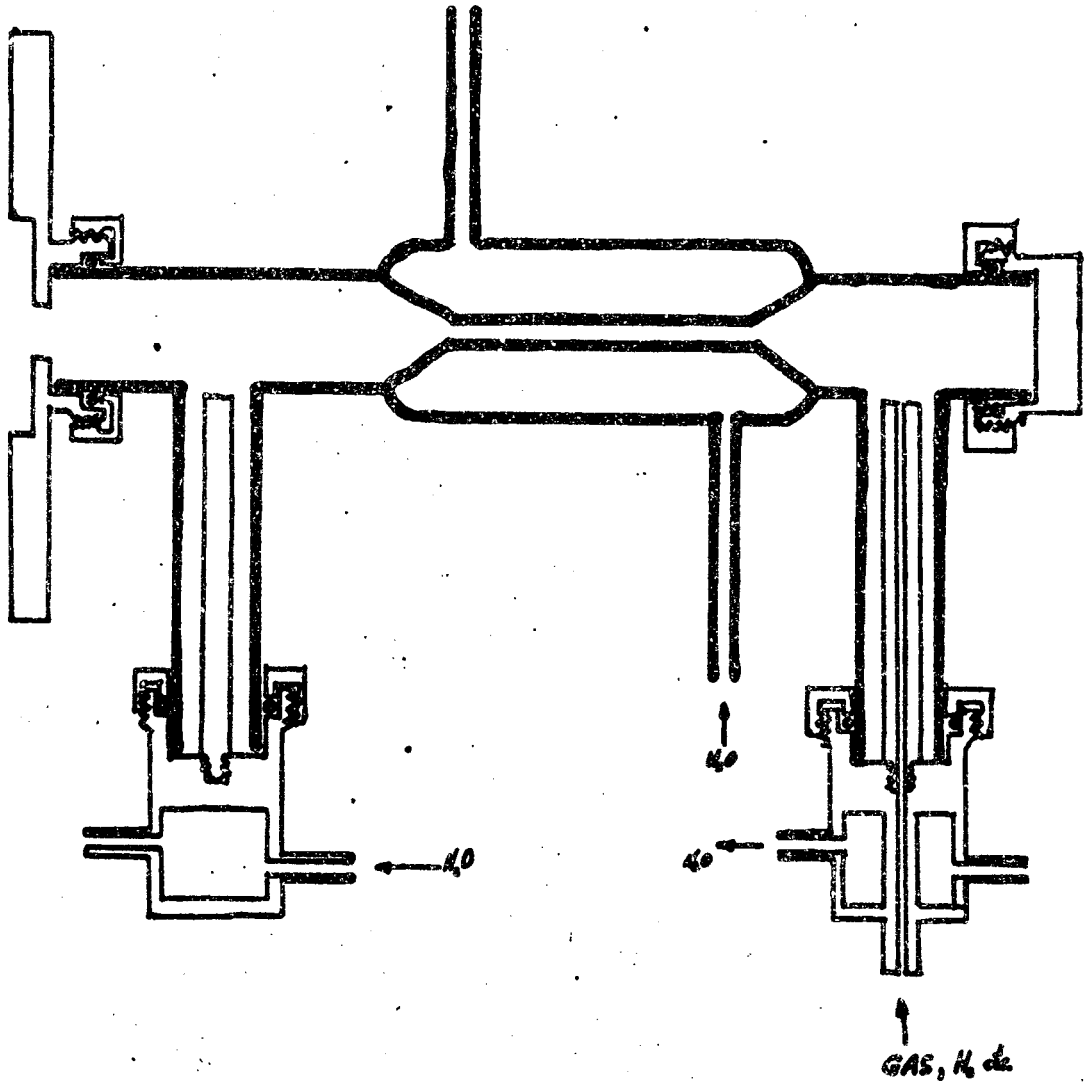

FIGURE 6. The light source.

amplifiers of the photocell circuit. The neon and helium resonance lines at 736Å and 584Å as well as the hydrogen many-lined molecular spectrum from 1608Å to 900Å were used to measure both the quantum yield and energy distributions. When using hydrogen, the tube was operated at a pressure of about 0.5 torr. The voltage across the discharge was about 620 volts with currents of 0.2 to 0.3 ampere. Helium and neon were used at pressures of approximately 0.2 torr; and for currents of about 0.3 ampere, the voltage drop was about 400 volts.

C. Sample Preparation

A piece of high purity indium was placed in the aluminum holder and as it was necessary that nothing but the indium be exposed to the light beam in the photocell, the entire end of the aluminum holder was coated with indium. The sample end of the sample holder was slipped into a hole which had been drilled in a piece of teflon and which was the size of the outside diameter of the aluminum sample holder itself. This prevented the indium from spilling over the side of the sample holder, thus insuring that there was an adequate thickness of indium for shaping and polishing. The sample, mold, and holder were then heated to about 160°C. whereupon the indium melted and flowed into the desired shape. Teflon was used because indium does not wet it and it

is stable up to 200°C. or more.

After the sample cooled, the mold was removed and the end of the sample was machined flat. The sample was then electropolished with a solution of one part concentrated nitric acid in three parts methanol. The indium to be polished formed the anode and a piece of sheet stainless steel was used as the cathode. It appeared that a current density of about 0.5 ampere/cm^2 was most effective; larger current densities tend to produce pits in the polished surface. The solution became yellow in color at the indium surface within about a second after the current was turned on. When this occurred, the polishing process was slowed markedly. To reduce the polishing time the current was turned on for about one second every three to five seconds and this current cycling was continued until the sample surface was highly polished. The sample and mount were then removed from the polishing tank and rinsed with methanol. The sample was then mounted in the photocell which was evacuated as soon as possible to minimize the oxidization of the sample.

D. Reflectivity Measurements

The experimental apparatus and procedure employed in measuring the reflectivity of solids including indium have been described in detail in references 10

and 11, so only the important features will be described here. The sample, polished as described in the preceding section, was formed by flattening the indium between two glass plates and polishing the flattened portion. A recording of the incident spectrum was made using a sodium salicylate coated light pipe and photomultiplier similar to the one described in section IIA of this paper. This was done with the sample raised out of the light path. After scanning and recording the spectrum once, the sample was lowered into the light beam. The sample holder was designed so that the light beam made a 20 degree angle with the normal to the sample's surface. The light pipe was rotated to intercept the reflected beam and a recording was made of the reflected intensity. The incident beam and reflected beams were re-measured alternately several times and the averarages of the several measurements of each were used to compute the reflectivity.

E. Quantum Yield

The quantum yield measurements were made by comparing the saturated photocurrent of the photocell with the current output of an EMI 6256B photomultiplier, operating at a fixed voltage, which monitored, through a light pipe, the phosporescent radiation of a sodium salicylate screen. The photocell current and the photo-

multiplier current were measured with a Keithley model 417 picoammeter. The photomultiplier voltage was provided by a Fluke model 412A regulated high voltage d-c supply. The output of the picoammeter was recorded with a Leeds and Northrup Speedomax G chart recorder. The measuring system is shown schematically in Fig. 7. The quantum yield measurements were made using 200μ slits giving a 1.6 Å band pass.

With the sample mounted in the evacuated photocell and a fresh layer of sodium salicylate on the light pipe, the light pipe was rotated to a position in which it gave the maximum signal. This was done at any convenient spectral line. The grating was then rotated to the short wave length end of the spectrum, and the scanning drive was set at 25 to 50 A/minute. After the incident spectrum was recorded, the light pipe was rotated out of the light path. With about 15 volts across the photocell to assure the collection of all photoelectrons, the spectrum was re-scanned and the photocell current recorded. According to several investigators (references 12, 13 and 14), the quantum yield of sodium salicylate is nearly unity and is practically constant throughout the vacuum ultraviolet, hence the output of the photomultiplier was assumed to be proportional to the incident light intensity. The

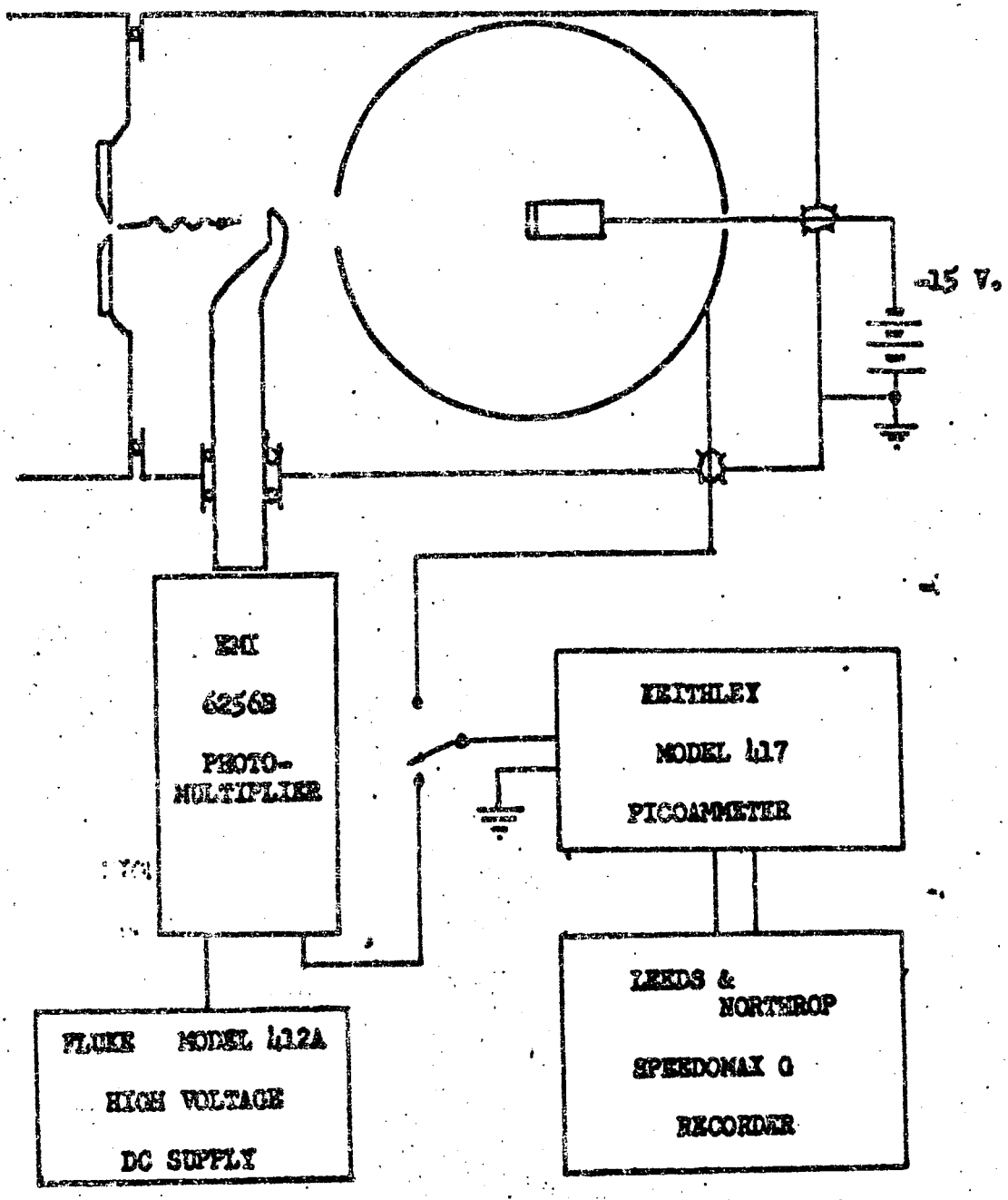

FIGURE 7. The components used in measuring the quantum yield.

relative quantum yield was calculated according to the relation,

$$Y = i_{pc}/i_o(1-R)$$

where i_{pc} is the photocell current, i_o is the photomultiplier current (incident light intensity), and R is the reflectivity.

F. Energy Distribution Measurement

A block diagram of the electronic components used in measuring photoelectron energy distributions is given in Fig. 8. The a-c signal was provided by a PAR (Princeton Applied Research) model JB-4 lock-in amplifier. The amplitude where possible was chosen to be 0.1 volts peak-to-peak to give good energy resolution in the energy distribution measurements. The operating frequency of 14 cps was selected to reduce the amplitude of the signal that was conducted capacitively by the photocell. The capacitance of this photocell was about 10^{-12} farad which gave a conductance of 10^{-10} mho at 14 cps. The maximum conductance due to photoemission from the most intense lines was about 2×10^{-10} mho.

A d-c sweep voltage was provided by a 45 volt battery connected across the ends of a 50,000 ohm ten-turn heli-pot with a fixed center tap. The a-c signal from the PAR was fed into the fixed center tap, and the combined a-c and d-c voltages appeared at the sliding

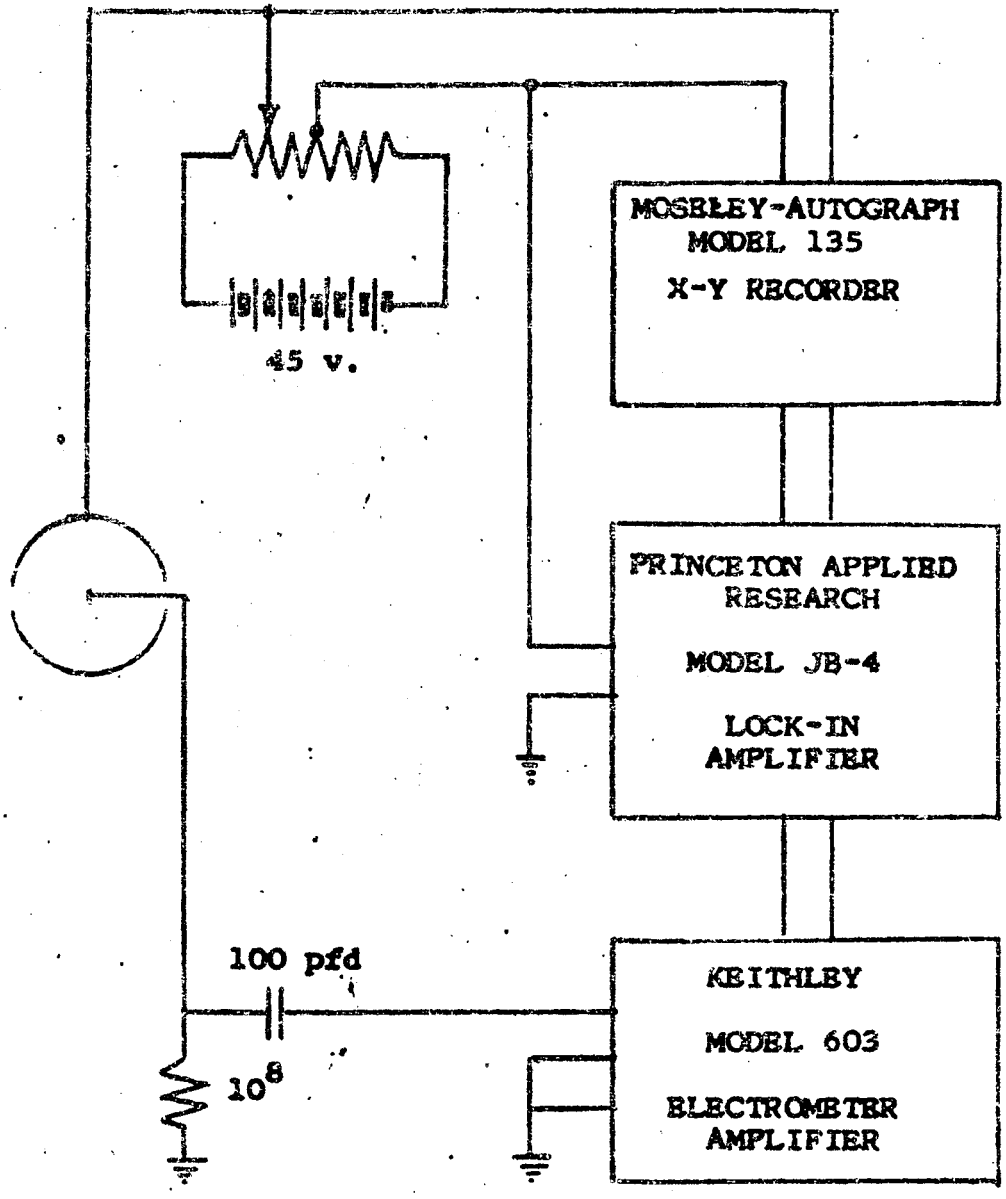

FIGURE 8. Block diagram of the components used in measuring photoelectron energy distributions.

tap of the heli-pot, which was connected to the collector of the photocell. The sliding tap was driven through a sequence of reduction gears by a 13 rpm clock motor. The d-c voltage was swept at about 0.5 volt/minute. The voltage between the sliding tap and the center tap was fed into the x-axis input terminals of a Moseley-Autograph model 135 x-y recorder. The voltage drop across the photocell output resistor was neglected since it was never more than 2% of the total voltage across the photocell.

The photocurrent was measured at the emitter, utilizing the collector as additional electrostatic shielding. Since only the a-c portion of the photocurrent was of interest in this measurement, the photocurrent was passed through a resistor to ground and the emitter was capacitively coupled to the input of a Keithley model 603 electrometer amplifier. A 10^8 ohm resistor was used for wave lengths having larger saturated photocurrents (5×10^{-11} amp and more) and 10^9 ohms for the smaller ones. A 10^8 ohm resistor gave a signal amplitude of 1 millivolt peak-to-peak when the photocell had a conductance of 10^{-10} mho and an input signal of 0.1 volts peak-to-peak was used. A 100 picofarad coupling capacitor and a grid resistor of 10^9 or 10^{10} ohms were used in the remote head of the electro-

meter amplifier. The electrometer amplifier had selectable gains of 10, 20, 40, 100, ..., and 4000. It also had a differential input which could be used to remove the capacitive signal conducted by the photocell when necessary (when the capacitive signal was 30 or more times larger than the photoelectron conductance). This was accomplished as shown in Fig. 9 with resistors R_1 and R_2 having equal values and the capacitor C adjusted to have the same capacitance as the photocell. For this work, it was not necessary to use the differential input.

The signal from the electrometer amplifier contained both the capacitive and the photoelectric signals but the phase difference between these two signals was exactly 90 degrees. By feeding the electrometer amplifier directly into the PAR amplifier, which acted as a phase sensitive detector, only that portion of the signal which was due to the photoelectric small-signal conductance of the photocell was measured. The phase of the PAR amplifier was adjusted by blocking off the light entering the photocell and adjusting the phase control to give zero output. This assured that only the photoelectric contribution to the a-c conductance was measured since the a-c conductance in the absence of light was almost entirely capacitive.

In order to record the final signal, the output of

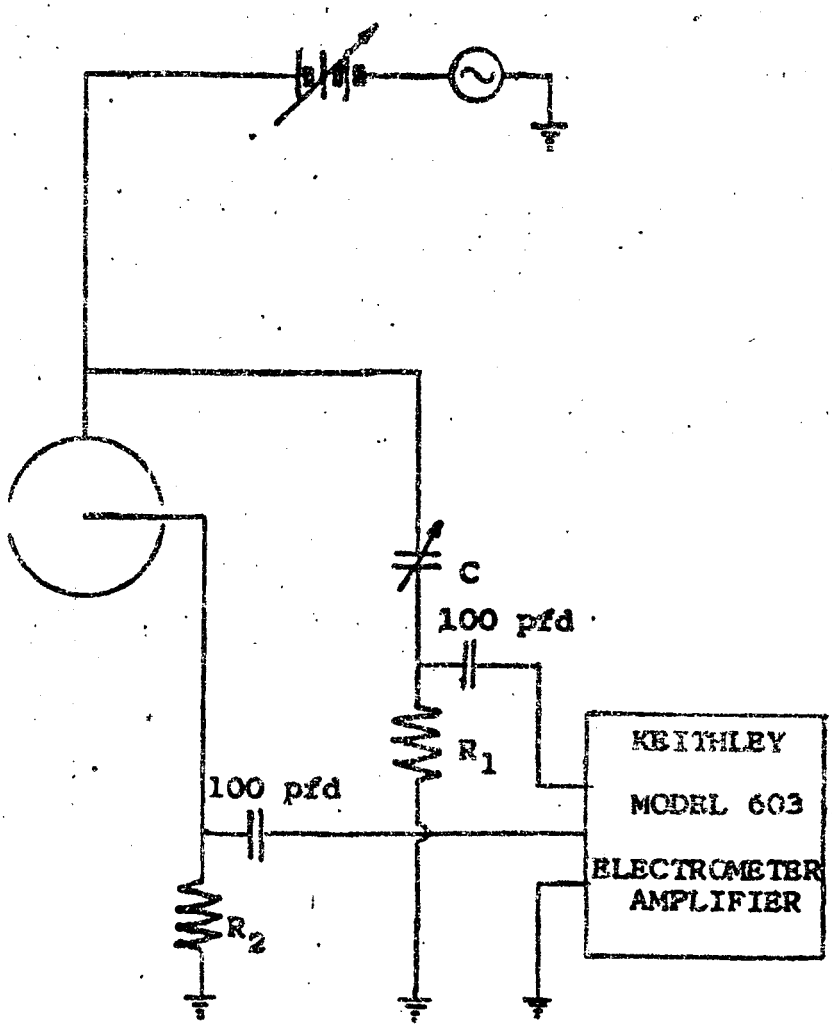

FIGURE 9. The differential input circuit used for low level signals.

the PAR amplifier was fed into the y-axis input of the x-y recorder. Energy distributions were then plotted directly by sweeping the d-c voltage.

III. Results and Conclusions

A. Reflectivity of Indium

The reflectivity of electropolished indium between 3.2 eV and 25 eV (4000 A to 500 A) is shown in Fig. 10. At 3.2 eV the reflectivity was 90% and it decreased rapidly to a sharp minimum of 42% at 6.0 eV and then increased to 47% at 6.5 eV. Following this peak the reflectivity fell rapidly again to a broad minimum at about 12.5 eV where it was down to 4%. It then displayed a very broad maximum centered at 17 eV after which it dropped slowly to 1% at 25 eV.

The structure in the reflectivity curve of a metal is generally due to intra-band transitions, inter-band transitions and plasma oscillations. In the present case, the peak at 6.5 eV may be due to a reduced plasma oscillation or inter-band transition (more work would be needed to determine the nature of the mechanism), while the sharp decrease in the reflectivity near 11 eV indicates the presence of a plasma frequency of this value. This agrees with the fact that thin films of indium exhibit an onset of transmission at 11.1 eV. The broad peak at 17 eV is due possibly to an inter-band transition and seems to be correlated with the sharp decrease in transmission found in thin films of indium at 16.8 eV.

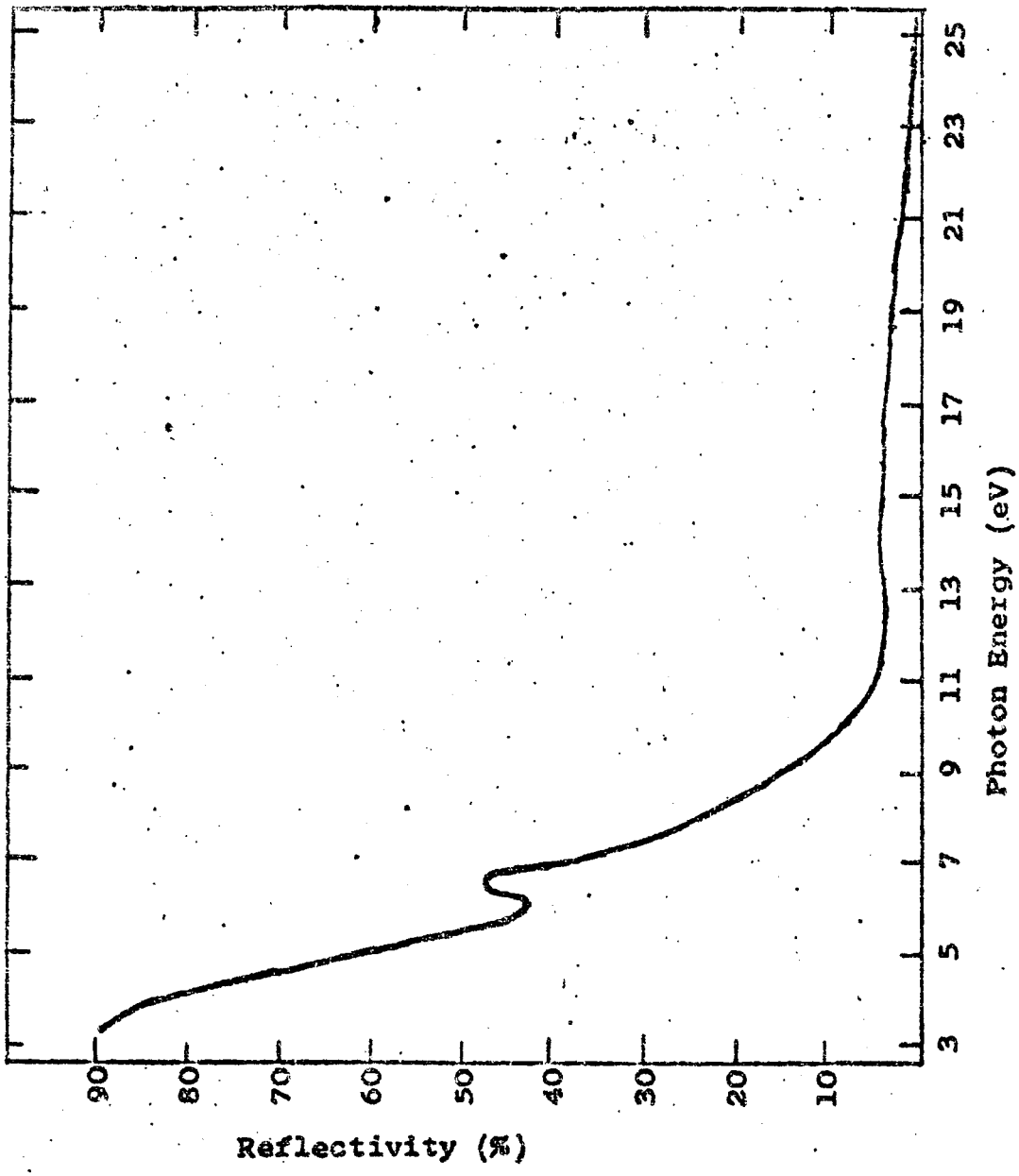

FIGURE 10. The reflectivity of indium.

B. Relative Quantum Yield of Indium

The absolute value of the intensity of the light beam was not determined and hence only the relative quantum yield was measured. The values obtained were adjusted so that the yield as given in Fig. 11 agreed with the quantum yield of indium at 13.1 eV as measured by Watanabye et al (ref. 15). It seemed best to adjust the relative quantum yield curve at the highest possible photon energy because the yield is less strongly influenced by any surface effects at higher energies.

The yield increased nearly exponentially from .008% at 7.7 eV to 1.0% at 10.2 eV whereupon it began increasing less rapidly until it reached 12% at 14.2 eV. At 16.6 eV it was 18%, 17.5% at 16.9 eV, and 15% at 21.2 eV. The fact that the yield increases exponentially near the threshold indicates that the observed photoemission is not characteristic of bulk indium in this region. The yield is expected to increase proportionally to the square of the photon energy for direct transitions, and to the two-thirds power of the photon energy for indirect transitions (ref. 16).

C. Indium Photoelectron Energy Distributions

In Fig. 12, typical energy distributions of photoelectrons from indium are shown for photon energies of 10.2, 12.1 and 14.1 eV. Fig.13 gives the energy

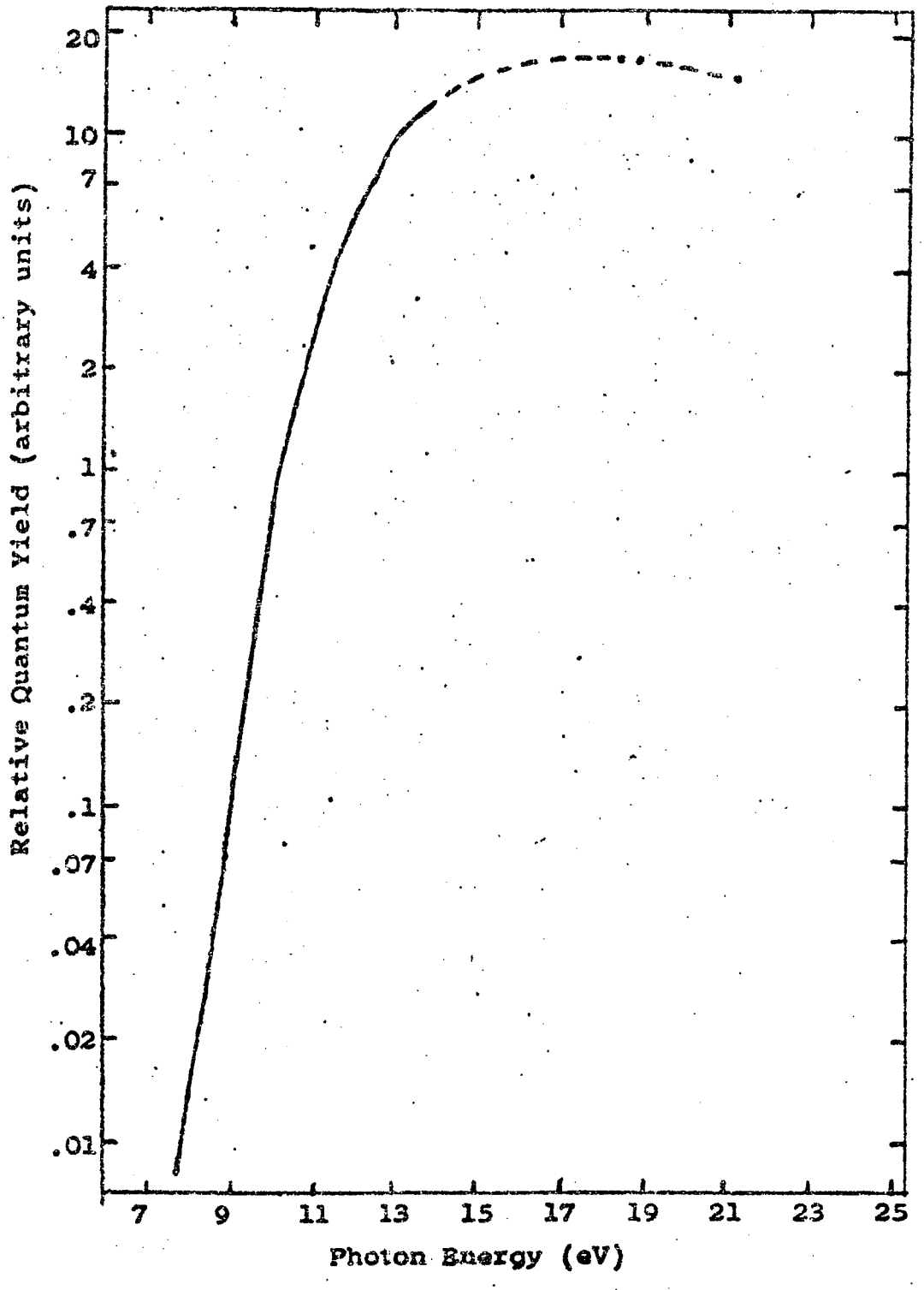

FIGURE 11. The relative quantum yield of indium.

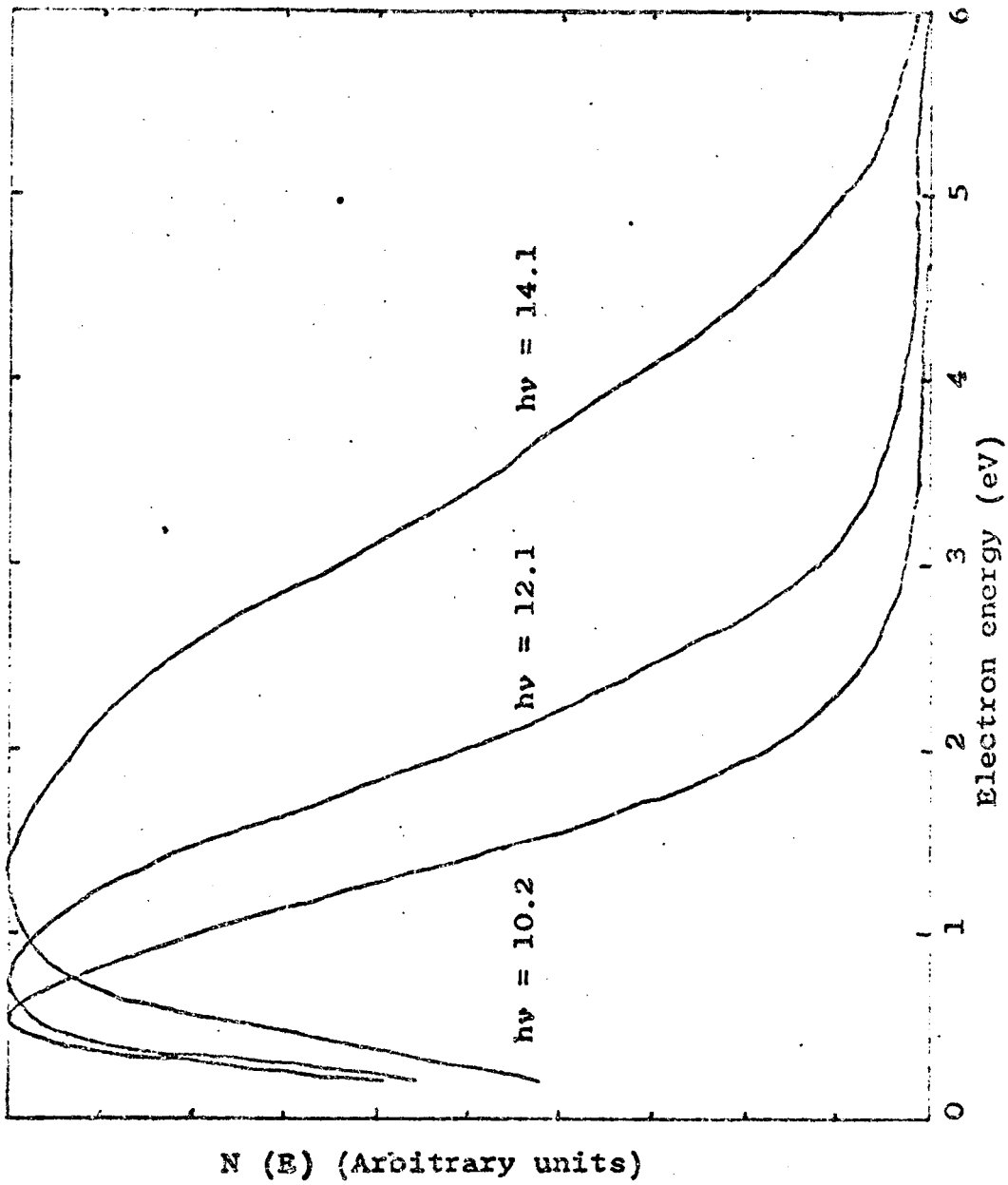

FIGURE 12. Photoelectron energy distributions from indium for photon energies of 10.2 eV, 12.1 eV, and 14.1 eV.

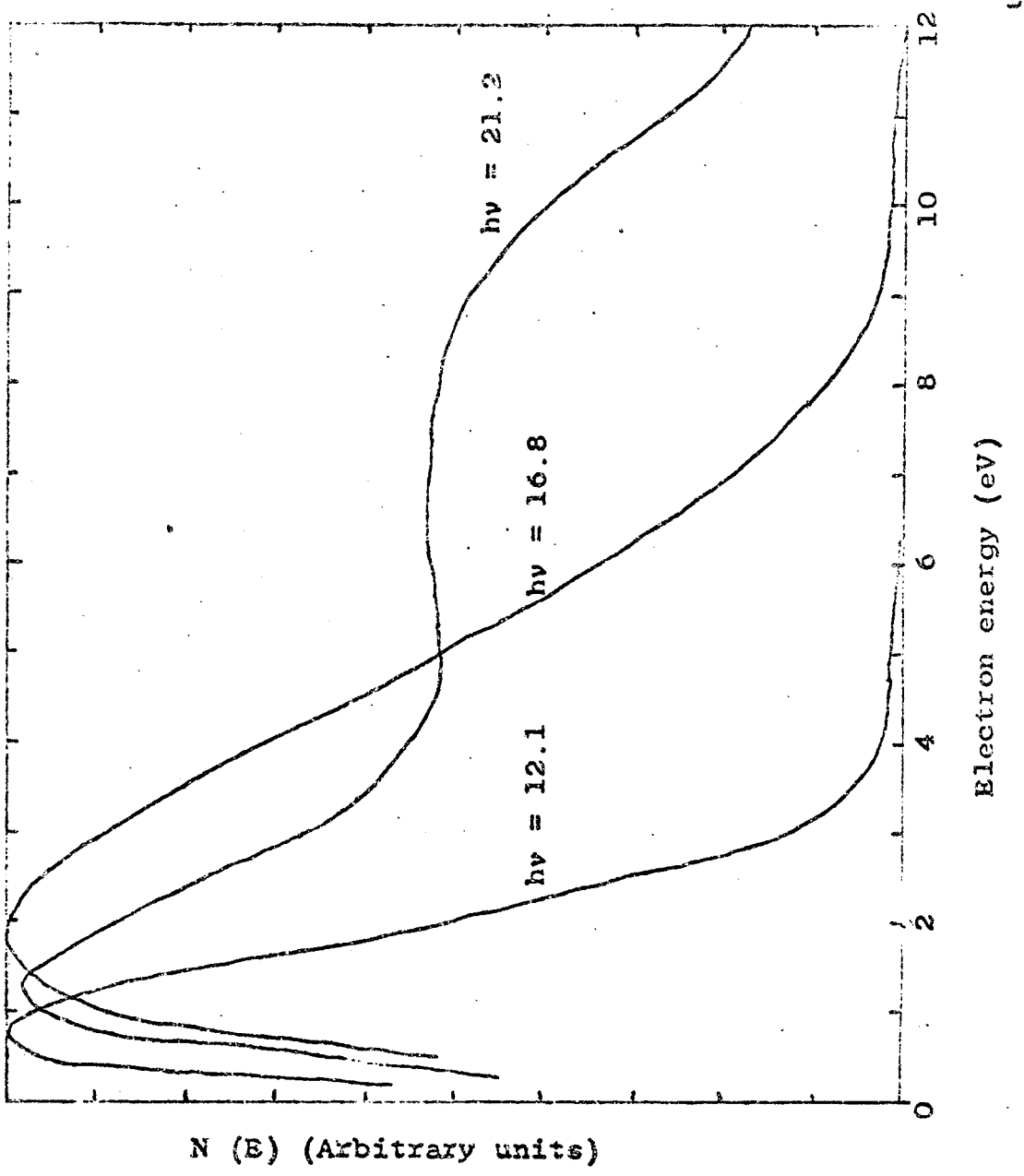

FIGURE 13. Photoelectron energy distributions from indium for photon energies of 12.1 eV, 16.8 eV, and 21.2 eV.

distributions for 12.1, 16.8 and 21.2 eV photons. Energy distributions were obtained also for photons of 7.7, 9.3, 9.7, 10.7, 11.2, 11.8, 12.6, and 13.5 eV; but since they follow the trend of those shown for 10.2 to 16.8 eV photons, they were not reproduced here. The energy distribution curves shown in Fig. 11 & 12 were measured three to five times for one sample and no apparent discrepancies noted. It is felt, therefore, that these distributions are characteristic of electropolished indium.

All of the distributions measured except that for 21.2 eV photons followed the same pattern. There was a strong peak at low energies which moved to higher energies as the photon energy increased but this exhibited no linearity with photon energy. Following the peak, $N_\omega(E)$ decreased rapidly to about 10% of the maximum and then slowly approached zero. The approximate energies at which the energy distributions went to zero did not seem to bear any simple relation to the photon energy except that as the photon energy increased, the energy at which $N_\omega(E)$ went to zero moved to higher energies.

The energy distribution for 21.2 eV photons had a peak at 1.3 eV followed by a minimum at 4.9 eV. Following the minimum there was a broad peak whose maximum lay

at 7.0 eV.

The absolute zero of photoelectron energies was taken to be -0.2 volt as this was the voltage toward which $N_w(E)$ tended to zero for all photon frequencies investigated. One expects for a metal that photoelectrons with nearly zero energy will occur since photoelectrons can be scattered before leaving the sample to states just above the vacuum level, even when there are no states at the energy of the incident photon below the vacuum level. The contact potential difference between the electro-polished indium emitter and the evaporated film of indium which served as a collector was therefore -0.2 volts. This contact potential difference is not overly large, considering the differences between the methods of the collector-emitter.

D. Conclusions

1. Method of Measurement.

The a-c method for obtaining photoelectron energy distributions utilizing the electronic components described herein is very effective. The results obtained in this study have demonstrated the applicability of the a-c direct-recording technique for obtaining photoelectron energy distributions of solids for photon energies far into the ultraviolet. The main limitation to the usefulness of the technique seems to be

the lack of intense spectral lines produced by the d-c light source employed. Extension of the technique to shorter wavelengths awaits improved noise-free sources of intense far ultraviolet radiation. During the course of the measurements it became clear that several important questions concerning the basic interactions, e. g., plasmon creation by high energy photoelectrons, can only be answered by studies using photons having energies in excess of 20 eV.

There are no particular difficulties in measuring conductances as low as 10^{-11} mho. For conductances less than this, perhaps down to 5×10^{-13} mho, useful information can be obtained by using the differential input of the electrometer amplifier. At conductances of about 10^{-11} mho, fluctuations due to noise were on the order of 5×10^{-12} mho (without using the differential input). An improvement in the system could be made by using a lock-in amplifier which would have the capability of handling lower frequencies (e.g., the PAR model JB-5 is useful to 1.5 cps as compared with the 15 cps limit of the JB-4 used in this work).

The photocell would be greatly improved by the addition of an evaporation filament to permit the application of the collector film in the photocell itself without necessitating the exposure of the collector

film to air. In addition, the sample surface could be obtained by evaporating the sample onto a suitable substrate. Another method for improving the sample surface -- at least for the softer metals such as indium -- would be to scrape the photo surface in the photocell and thereby expose a clean surface under high vacuum.

2. Interpretation of the Results on Indium.

The present study was primarily concerned with perfecting a workable measuring technique for future application to band structure studies in solids so that only preliminary results were obtained for indium. Since no other measurements of comparable range and accuracy exist for indium, the main features of these results are of sufficient interest to deserve a brief attempt at an interpretation.

The energy distribution curves for indium are about what one would expect -- except for the 21.2 eV curve -- for a metal exhibiting only intra-band transitions in the photon energy range covered, except for the apparent lack of photoelectrons with energies near the photon energy minus the work function, that is, hν-4eV. Whereas it might be thought that this feature is due to a very low density of initial states near the Fermi level in indium, this is not

the case, because the spread of missing energies becomes larger as the photon energy increases. It is felt that this feature of the energy distributions as well as the logarithmic increase in quantum yield for these samples is probably a result of scattering of photoelectrons from surface impurities and defects introduced by the methods used to prepare the samples.

The broad secondary peak at 7 eV in the energy distribution for 21.2 eV photons, although interesting, is difficult to interpret at present. At a photon energy of 21 eV, an unscattered photoelectron whose final state energy is 7 eV above the vacuum level would have been excited from a state lying 10 eV below the Fermi level (assuming a 4 eV work function). This does not correspond to any known maximum in the density of states of indium as can be seen by an examination of the reflectance curve given in Fig. 9. Information is needed about energy distributions for several photon energies near 21.2 eV in order to clarify the nature of the structure observed. It was not possible to obtain energy distributions for photon energies near 21.2 eV as no source of strong, noise free radiation is available in this region of the spectrum except the helium resonance line at 21.2 eV.

It is presumably possible for electrons which have

been excited to an energy above the vacuum level (equal to the plasma energy) to lose this energy by exciting a plasmon. In the case of indium (a metal well suited for the observance of this phenomenon because of its well defined plasma oscillation) the plasma energy is 11.1 eV and the work function is about 4.1 eV. This indicates that any secondary excitation of plasmons by photoelectrons would not occur for photon energies less than 15.2 eV. Unfortunately there are no usable spectral lines between 14.2 eV and 16.6 eV with our present light source and hence the quantum yield as measured here does not offer any information as to whether or not secondary excitation of plasmons occurs. Furthermore, the only energy distribution curve with electron energies up to and greater than 11 eV is that obtained for 21.2 eV photons. This distribution exhibits a decrease in the vicinity of 11 eV but it is felt that this is insufficient evidence to permit the assertion that secondary excitation of plasmons is occuring. If energy distributions for higher energy photons should show a decrease at 11 eV it can be concluded that plasma excitations are perhaps being observed. Until this information is obtained, however, the question of the observability of secondary excitation of plasmons by photoelectrons remains unanswered.

List of Illustrations

References

1. W. E. Spicer and R. E. Simon, J. Phys. Chem. Solids, 23, 1817, (1962).

2. G. W. Gobeli and F. G. Allen, Phys. Rev., 127, 141, (1962).

3. G. W. Gobeli and F. G. Allen, Phys. Rev., 127, 150, (1962).

4. E. A. Taft and H. R. Philipp, Phys. Rev., 115, 1583, (1959).

5. W. E. Spicer, Phys Rev., 112, 114, (1958).

6. W. E. Spicer, J. Appl. Phys., 31, 2077, (1960).

7. W. E. Spicer and R. E. Simon, Phys. Rev. Lett., 9, 385, (1962).

8. N. E. Kindig, Band Structure and Surface Effects in Cadmium Sulfide Photoemission Studies, Stanford Electronics Laboratories Technical Report No. 5201-1, (1964).

9. C. N. Berglund, Band Structure and Electron-Electron Scattering in Copper and Silver, Stanford Electronics Laboratories Technical Report No. 5205-1, (1964).

10. J. F. Osantowski, Reflectivity of Solids in the Vacuum Ultraviolet, (M. A. Thesis) University of California, Santa Barbara, (1963).

11. A. J. Al Kezweeny, Extreme Ultraviolet Photon Absorption in Metals, (M. A. Thesis) University of California, Santa Barbara, (1962).

12. N. Wainfan, W. C. Walker, and G. L. Weissler, J. Appl. Phys., 24, 1318, (1953).

13. A. M. Smith and D. Dutton, J. Phys. Chem. Solids, 23, 315, (1961).

14. J. A. R. Samson, J. Opt. Soc. Am., 54, 6, (1964).

15. K. Watenabye, F. M. Matsunaga, and R. S. Jackson, Some Intensity Measurements in the Vacuum Ultraviolet, University of Hawaii Press, (1964).

16. E. O. Kane, Phys. Rev., 127, 131, (1962).